Soft-x-ray microscopy using spiral zone plates

Anne Sakdinawat[1,2,*] and Yanwei Liu[2]

[1]*University of California San Francisco and University of California Berkeley Joint Graduate Group in Bioengineering, University of California, Berkeley, California, 94720, USA*

[2]*NSF ERC for Extreme Ultraviolet Science and Technology, University of California Berkeley, and Center for X-ray Optics, Lawrence Berkeley National Laboratory, Berkeley, California 94720, USA*

**Corresponding author: aesakdinawat@lbl.gov*

Received June 14, 2007; accepted July 19, 2007;
posted July 31, 2007 (Doc. ID 84154); published September 4, 2007

Phase sensitive soft-x-ray microscopy methods enable the study of specimens for which phase effects are a prevalent contrast mechanism. One way to detect these phase effects is to optically implement the radial Hilbert transform by using spiral zone plates (SZPs), which results in the isotropic measurement of the amplitude and phase gradient in a sample. Soft-x-ray microscopy using an SZP as a single element objective lens was demonstrated through the imaging of a 1 μm circular aperture at a wavelength of 2.73 nm (454 eV). A regular zone plate, a charge 1 SZP, and a charge 2 SZP were fabricated using electron beam lithography and were used as the imaging optic in the microscopy setup. The charge 1 and charge 2 SZP images exhibited isotropic edge enhancement as a result of radial Hilbert filtering. © 2007 Optical Society of America

OCIS codes: 070.6110, 340.7460, 050.1970.

Phase sensitive techniques for x-ray microscopy are useful for enhancing contrast because many samples in this regime are primarily phase objects, especially at higher energies (hard x rays) where many objects have little amplitude contrast and also at lower energies (soft x rays) when objects are probed away from absorption edges. Phase sensitive imaging methods such as Zernike phase contrast [1], phase contrast interferometric imaging [2], and differential interference contrast [3,4] have been implemented for x-ray microscopy. Recently, unidirectional phase sensitivity was demonstrated using an XOR pattern in a soft-x-ray microscope [5]. Radial Hilbert transform imaging provides an isotropic phase sensitive method that measures the gradient of the complex refractive index of an object [6] and has been implemented in the visible light regime using spiral zone plates (SZPs) [7,8], forked gratings [9,10], and spiral phase plates [11]. In the x-ray regime x-ray vortices have been generated using spiral phase plates [12] and high topological charge SZPs [13]. The objective of this Letter is to demonstrate isotropic sensitivity by performing both imaging and the radial Hilbert transform at soft-x-ray wavelengths using the SZP as a single element objective.

Using an SZP as a single element objective is equivalent to optically performing the radial Hilbert filtering operation and the imaging operation in a single step. The radial Hilbert phase function is given by

$$H_p(r,\phi) = \exp(ip\phi), \tag{1}$$

where p represents the topological charge and r,ϕ are the polar coordinates. The zone plate (ZP) phase function is given by

$$\mathrm{ZP}(r,\phi) = \exp\left(\frac{-i\pi r^2}{\lambda f}\right), \tag{2}$$

where λ is the wavelength and f is the focal length of the ZP lens. The SZP is obtained by multiplying the radial Hilbert phase function with the ZP phase function and is given by

$$\mathrm{SZP}_p(r,\phi) = H_p(r,\phi)\mathrm{ZP}(r,\phi) = \exp\left(ip\phi - \frac{i\pi r^2}{\lambda f}\right). \tag{3}$$

Due to fabrication constraints for diffractive optics in the x-ray regime, SZP phase representations are binarized, resulting in ZPs as shown in Fig. 1. Like a regular ZP, the SZP is chromatic, requiring a relative spectral bandwidth less than 1/number of zones, and image formation, just as in conventional soft-x-ray microscopy, is performed using the first order of the zone plate.

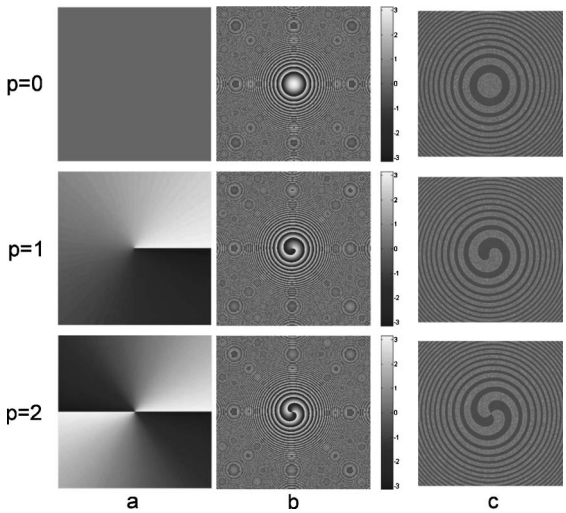

Fig. 1. a, Computer-generated radial Hilbert transform phase structures; b, computer-generated SZP phase structures; c, SEM images of the central portions of the binarized SZPs fabricated for the imaging experiment. The ZP parameters were as follows: outermost zone width of 72 nm, diameter of 86.7 μm, 300 zones, 240 nm thick nickel.

Because the SZP combines the radial Hilbert filtering operation and imaging in a single step, it can be used as a single optical element as long as conditions for both the filtering and imaging operations are satisfied at a single plane. The condition for implementing radial Hilbert filtering as a Fourier filter is that the Fourier transform of the sample is incident upon the optic. The imaging condition is that the focal length, sample to optic distance, and optic to image distance satisfies the Gaussian lens equation. One setup that satisfies these requirements is to set the sample-to-optic distance equal to the length required for the Fraunhofer diffraction of a certain field of view of the object, and to then set the optic to image distance as required by the Gaussian lens equation. For high magnification setups common in x-ray microscopes, the sample-to-optic distance is close to the focal length of the imaging optic. The largest aperture area that satisfies the Fraunhofer approximation for a given wavelength determines the field of view. An alternative setup that also generates the Fourier transform of the object at the plane of the SZP is to illuminate the sample with a converging beam [14]. This has the advantage of decoupling the sample to an optic distance from the focal length, allowing a smaller sample to the optic distance and allowing higher magnification at more reasonable working distances. Larger fields of view and better resolution can be obtained with this setup. The disadvantage is that an additional optic increases the complexity of optical element alignment. The first of these two methods was implemented due to its simplicity and was used to demonstrate radial Hilbert filtering for soft x rays using a single optical element, the SZP.

Three types of ZP lenses were fabricated using electron beam lithography: a regular ZP, a charge 1 SZP, and a charge 2 SZP. Each of these was designed to have 300 zones, an outermost zone width of 72 nm, and a diameter of 86.7 μm. A 100 nm thick silicon nitride (Si_3N_4) membrane was used as the substrate for these ZPs. A plating base consisting of 5 nm chrome and 12 nm gold was evaporated onto the Si_3N_4, and hydrogen silsesquioxane (HSQ), a negative electron beam resist, was spun onto the wafer. The resist was patterned using the Nanowriter at the Center for X-ray Optics and was developed using a solution of tetramethylammonium hydroxide (TMAH). The wafer was then electroplated with 240 nm thick nickel, and the remaining resist was stripped in a buffered hydrofluoric acid solution. The material selection and thickness were designed to optimize the first-order diffraction efficiency for imaging at water window energies ($\lambda = 2.4-3$ nm). Scanning electron microscope (SEM) images of the optics are shown in Fig. 1.

The ZPs were used in the radial Hilbert transform imaging experiment performed with beamline 12.0.2.1 at the Advanced Light Source (ALS) in Berkeley [15]. The experimental setup is shown in Fig. 2. The third harmonic of an 8 cm undulator was used to generate soft x rays from 200 eV to 1 keV. The wavelength of the radiation was tuned to 454 eV (2.73 nm) with a spectral bandwidth of $\Delta\lambda/\lambda = 1/500$ using a

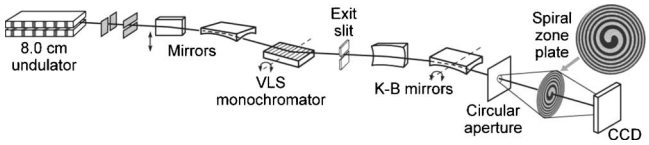

Fig. 2. Schematic of the beamline and microscope setup.

varied line-space (VLS) plane grating monochrometer. The beam was then focused into the experimental chamber to a final spot size of 80 μm $\times$ 10 μm FWHM (horizontal $\times$ vertical) using a pair of tungsten-coated Kirkpatrick–Baez mirrors. A 1 μm circular aperture was placed at the focus of the beam and served as the sample that was imaged. The transverse coherence length at the aperture plane was previously shown to be $\sim$4 μm [15], so the 1 μm aperture was coherently illuminated and its Fourier transform was obtained at the imaging optic (regular zone plate or SZP) 2.29 mm away. All of the ZPs were designed with a first-order focal length of 2.28 mm at a wavelength of $\lambda = 2.73$ nm, and the CCD was placed downstream of the ZP to provide 425 times magnification.

Soft-x-ray imaging of a 1 μm circular aperture using the three aforementioned ZPs is shown in Fig. 3. The image taken with a regular ZP shows uniform intensity distribution throughout the circular aperture

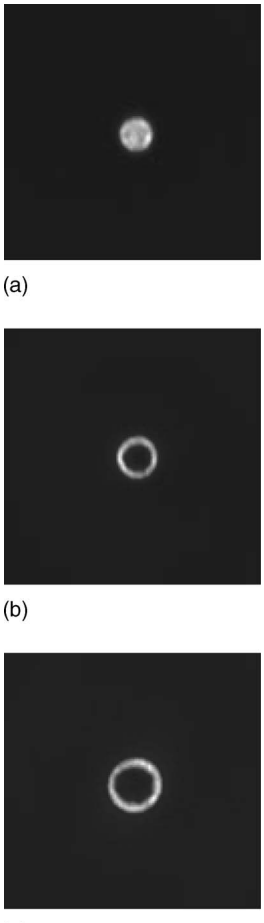

Fig. 3. Images of a 1 μm circular aperture taken at a wavelength of $\lambda = 2.73$ nm with each of the ZPs: (a) regular, (b) charge 1 spiral, (c) charge 2 spiral.

with some ringing effects at the edges as expected from highly coherent illumination. Both the images from the charge 1 and charge 2 SZPs show isotropic edge enhancement and intensity cancellation in the middle as a result of the radial Hilbert filtering. As the charge increases, the edge-enhanced image increases in size as seen in the comparison of image Fig. 3(b) with Fig. 3(c). This is due to the different phase filtering characteristics associated with SZPs of different charges [8]. The spatial resolution, as estimated from the width of the rings, is 150 nm for the charge 1 SZP and 235 nm for the charge 2 SZP, as expected from the 72 nm outmost zone width. Just as in conventional soft-x-ray imaging using a regular ZP, the resolution can be improved by fabricating a ZP with a smaller outermost zone width.

Soft-x-ray microscopy using SZPs was demonstrated at $\lambda = 2.73$ nm with both a charge 1 SZP and a charge 2 SZP. The images obtained using the two SZPs showed isotropic edge enhancement due to radial Hilbert filtering, demonstrating that SZPs can be used as a phase sensitive imaging method in the x-ray regime. Because the radial Hilbert filter is sensitive to changes in both the amplitude and phase of an object, imaging with a SZP can be used to detect the phase component of an object with a complex index of refraction. This can be used as a method of phase sensitive imaging, especially at higher x-ray energies where the amplitude contrast for most materials is small. For applications involving magnetic materials, x-ray magnetic circular dichroism imaging studies can be performed away from the absorption edges in a region where phase changes are dominant. For biological imaging, the additional phase sensitivity can provide enhanced contrast, leading to decreased exposure time and decreased radiation damage.

The authors gratefully acknowledge the contributions of E. Anderson, D. Attwood, K. Goldberg, E. Gullikson, S. Marchesini, R. Miyakawa, and P. Naulleau of Lawrence Berkeley National Laboratory and S. Bernet, S. Fürhapter, A. Jesacher, C. Maurer, and M. Ritsch-Marte of Innsbruck Medical University. This work was supported by the National Science Foundation Engineering Research Center (NSF ERC) for EUV Science and Technology, and by the U. S. Department of Energy (DOE), Office of Science, Basic Energy Sciences, Division of Materials Sciences and Engineering.

References

1. G. Schmahl, D. Rudolph, P. Guttman, G. Schneider, J. Thieme, and B. Niemann, Rev. Sci. Instrum. **66**, 1282 (1995).
2. C. David, B. Nöhammer, H. H. Solak, and E. Ziegler, Appl. Phys. Lett. **81**, 3287 (2002).
3. B. Kaulich, T. Wilhein, E. Di Fabrizio, F. Romanato, M. Altissimo, S. Cabrini, B. Fayard, and J. Susini, J. Opt. Soc. Am. A **19**, 797 (2002).
4. E. Di Fabrizio, D. Cojoc, S. Cabrini, B. Kaulich, J. Susini, P. Facci, and T. Wilhein, Opt. Express **11**, 2278 (2003).
5. C. Chang, A. Sakdinawat, P. Fischer, E. Anderson, and D. Attwood, Opt. Lett. **31**, 1564 (2006).
6. J. A. Davis, D. E. McNamara, D. M. Cottrell, and J. Campos, Opt. Lett. **25**, 99 (2000).
7. N. R. Heckenberg, R. McDuff, C. P. Smith, and A. G. White, Opt. Lett. **17**, 221 (1992).
8. K. Crabtree, J. A. Davis, and I. Moreno, Appl. Opt. **43**, 1360 (2004).
9. S. Fürhapter, A. Jesacher, S. Bernet, and M. Ritsch-Marte, Opt. Express **13**, 689 (2005).
10. C.-S. Guo, Y.-J. Han, J.-B. Xu, and J. Ding, Opt. Lett. **31**, 1394 (2006).
11. G. A. Swartzlander, Jr., Opt. Lett. **26**, 497 (2001).
12. A. G. Peele, P. J. McMahon, D. Paterson, C. Q. Tran, A. P. Mancuso, K. A. Nugent, J. P. Hayes, E. Harvey, B. Lai, and I. McNulty, Opt. Lett. **27**, 1752 (2002).
13. D. Cojoc, B. Kaulich, A. Carpentiero, S. Cabrini, L. Businaro, and E. Di Fabrizio, Microelectron. Eng. **83**, 1360 (2006).
14. J. W. Goodman, *Introduction to Fourier Optics* (McGraw-Hill, 1996).
15. K. Rosfjord, Y. Liu, and D. Attwood, IEEE J. Sel. Top. Quantum Electron. **10**, 1405 (2004).